Influence of grout material in shield tail on shield tunnelling performance

M. SUGIMOTO
Nagaoka University of Technology, Niigata, Japan

A. SRAMOON
TEAM Consulting Engineering and Management Co., Ltd., Bangkok, Thailand

H. IWASAKI
Nagaoka University of Technology, Niigata, Japan

ABSTRACT: When during tunnelling the shield advances forward, grout mortar is applied to fill the gap between the excavated surface and the extrados of the tunnel lining. The grout is sometimes intruded and hardened up in the shield tail and it might cause difficulty in controlling the shield tunnelling performance. Therefore, the aim of this study is to examine the influence of the intrusion of the grout on the shield tunnelling performance. This study examines the behaviour of the articulated shield during excavation a curved alignment. The simulation results revealed that the intrusion of the grout material into the shield tail is one of the factors affecting the shield behaviour during excavation.

1 INTRODUCTION

Articulated shield is increasingly adopted to use in curved tunnel construction in order to reduce the disturbance of ground around the shield, since conventional shield faced some difficulties in operational control of tunnel excavation and generated the wide range of the ground disturbance during excavation especially at sharp curves. General technique of the conventional shield to negotiate the curve is the use of the unsymmetrical jack pattern to generate the jack moment and the use of copy cutters to increase the excavated area in the ground. When this shield is employed at a sharp curve, the middle length of the shield at the inward of the curve and the shield tail at the outward of the curve push the surrounding ground, since the copy cutter length has some limitation to prevent the ground disturbance due to excess over cutting. This hampers the steering of the shield into the designated route. In order to overcome that problem, the shield is divided into two parts around the middle of its length and these two parts are connected by a rotating connection. This is so called articulated shield. The articulated shield can bend in any designed direction. However, it is usually designed to bend in the horizontal direction to make the horizontal curved tunnel.

Articulation of the shield is applied when the use of the copy cutter is not enough during excavation at the curve. The articulated shield is also employed to prevent an excess over cutting and to minimize the ground disturbance. Articulated jacks are placed between two sections of shield. Shield jacks are used to drive the shield advance, whereas articulated jacks are used to bend the shield during excavation. The angle between the axes of two sections of shield is called as articulated angle, which is predetermined based on the radius of the curve. The general feature of articulated shield is shown in Figure 1.

Grout mortar is applied to fill the gap between the excavated surface and the extrados of tunnel lining during shield advancement. Although the backfill

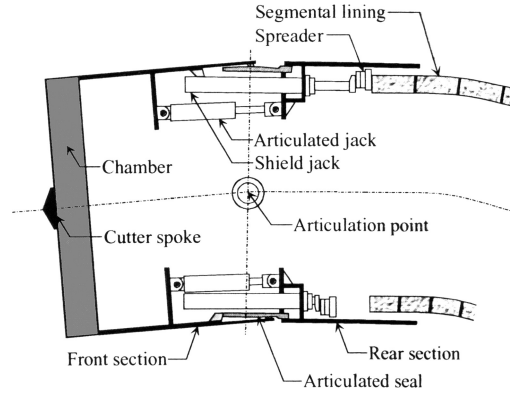

Figure 1. General feature of articulated shield.

grouting is skilfully controlled, the grout material is sometimes intruded and hardened up in the shield tail. This phenomenal especially occurs during the shield tunnelling at the curve alignment. The intrusion of the grout might cause the difficulty in control of the shield tunnelling performance.

To describe the articulated shield tunnelling characteristics as well as the influence of the intrusion of the grout on the articulated shield tunnelling performance, real time measurement data were obtained. The behaviour of the articulated shield tunnelling is simulated in order to examine causes and effects of grout mortar intrusion. The performance of articulated shield tunnelling is also discussed in this paper.

2 ARTICULATED SHIELD MODEL

The articulated shield model has been developed based on an existing model of a single circular shield (Sugimoto & Sramoon 2002) by dividing the model into two components, a front and rear section, at the centre of articulation. The loads acting on the articulated shield can be depicted as shown in Figure 2. The force due to self-weight of machine f_1 and the force on the shield periphery f_5 acts on both sections of the shield. Force at the shield tail f_2 acts only on the rear section, the shield tail, whereas the force at the face f_4 is loaded on the cutter disc on the front section. The force on jack thrust f_3 is composed of the forces due to the shield jack and the articulated jack.

The calculation procedures to obtain the forces are similar to those described in the previous model except only for the procedures to calculate f_3. Thus, only the procedures to calculate f_3 are presented in this paper. To calculate the shield jack force f_{31}, the direction of each shield jack has to be determined, since it is sometimes not parallel to the shield axis due to articulation of the shield. The direction of ith shield jack $\boldsymbol{e}_{SJi}$ can be determined from

$$\boldsymbol{e}_{SJi}^{T} = \frac{\boldsymbol{r}_{SJFi}^{T} - \boldsymbol{r}_{SJRi}^{T}}{\left| \boldsymbol{r}_{SJFi}^{T} - \boldsymbol{r}_{SJRi}^{T} \right|} \tag{1}$$

where $\boldsymbol{r}_{SJFi}$ and $\boldsymbol{r}_{SJRi}$ are the position vectors of the shield jack at the front end and at the rear end respectively.

$\boldsymbol{r}_{SJFi}$ is usually a pinned support, whereas $\boldsymbol{r}_{SJRi}$ is movable depending on the position of the last erected segmental lining inside the shield tail. The ith shield jack force $\boldsymbol{F}_{31i}$ can then be obtained as

$$\boldsymbol{F}_{31i}^{M} = A_{SJ} P_{SJi} \boldsymbol{e}_{SJi}^{M} \tag{2}$$

where A_{SJ} is the cross sectional area of the shield jack and P_{SJi} is the applied hydraulic jack pressure for ith shield jack.

The articulated jack force f_{32} is not necessary to calculate, since it is governed by the articulation angle θ_A and the summation of the force due to f_{32} is always zero. θ_A is determined prior to the excavation at the curve and the articulated jack force is always adjusted in order to attain the predetermined θ_A.

The articulated shield behaviours are obtained from the equilibrium of the forces acting on the shield, that is

$$\begin{bmatrix} \sum_{i=1}^{5} \left(\boldsymbol{F}_{Fi}^{M} + \boldsymbol{F}_{Ri}^{M} \right) \\ \sum_{i=1}^{5} \left(\boldsymbol{M}_{Fi}^{M} + \boldsymbol{M}_{Ri}^{M} \right) \end{bmatrix} = 0 \tag{3}$$

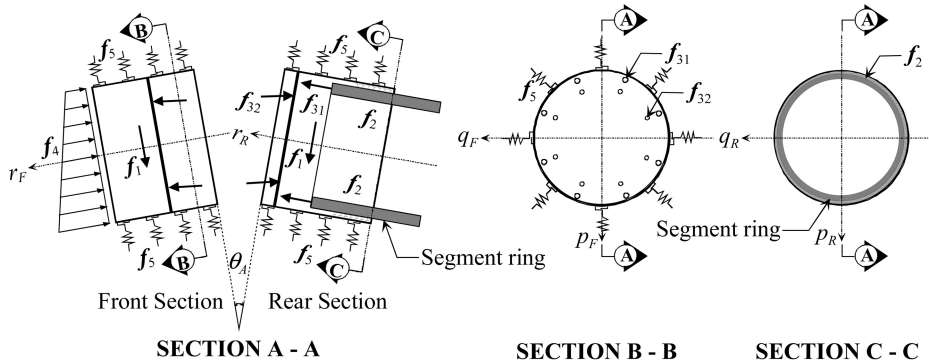

f_1 : self-weight of machine
f_2 : force on the shield tail
f_{31} : force due to the shield jack thrust
f_{32} : force due to the articulate jack thrust
f_4 : force acting at the face
f_5 : force acting on the shield periphery
θ_A : articulated angle

Figure 2. Model of loads acting on articulated shield.

where $\boldsymbol{F}$ and $\boldsymbol{M}$ are the force and moment vectors respectively and subscripts F and R denote front and rear sections of the shield respectively. The moment vector is generated by the cross product of the position and the force vectors. Here, notes that superscripts T and M indicate global and machine coordinate systems respectively, which can be transformed to other coordinate systems by using transformation matrices.

3 ARTICULATED SHIELD TUNNELLING PERFORMANCES

The tunnel test site was excavated by an articulated slurry shield with a 8.08 m outer diameter and 8.78 m length. Lengths of front and rear sections are 4.45 m and 4.33 m respectively. The diameter of segmental lining is 7.90 m and its standard width is 1.20 m.

The tunnel is laid in dense sand and stiff clay layers as shown in Figure 3. The overburden depth is approximately 25.5 m and the ground water table is 9.00 m below the ground surface. The horizontal radius of the left curve is 200 m and the analysis length of tunnelling is 70 m approximately.

The operational control during excavation, i.e., jack thrust, cutter torque, etc., was applied to control the shield to move on the planned alignment as shown in Figure 4. The applied jack thrust F_{31r} was in between 25 and 35 MN. The horizontal and vertical jack moments, M_{31p} (+: right hand rotation) and M_{31q} (+: downward rotation), were fluctuations during excavation, which were dependent on manipulation of the jacks by an operator. The cutter torque CT (+: clockwise rotation viewed from tail) to rotate the cutter disc was 2.0 MN-m approximately. The face pressure P_f was controlled in order to prevent the collapse of excavated face.

The copy cutters and articulation of the shield were applied together in order to negotiate the curve. The copy cutter CC and articulated angle θ_A were mostly applied in the horizontal direction, since the curve is in the horizontal direction. CC was approximately 2 cm in length and was applied in the range of 30° ∼ 150° (measured from the shield invert in the clockwise direction viewed from tail). θ_A was applied based on the assumption that both shield sections are laid along the curve. The applied articulated angle was gradually increased in horizontal direction until it reached the predetermined value which suited for the 200 m horizontal radius, and remained constant. CC and θ_A were not applied when the shield excavated in the straight alignments.

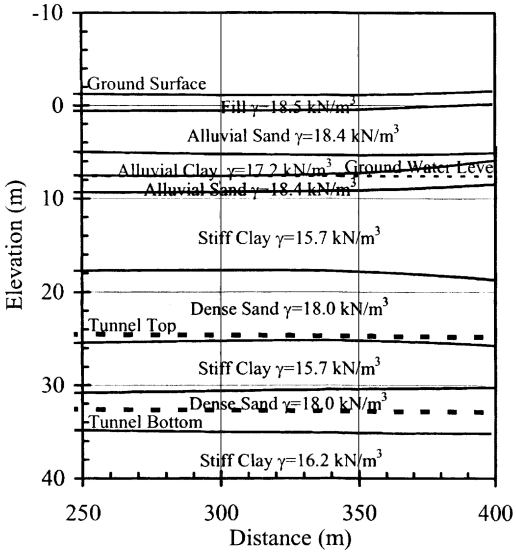

Figure 3. Geological profile at test site location.

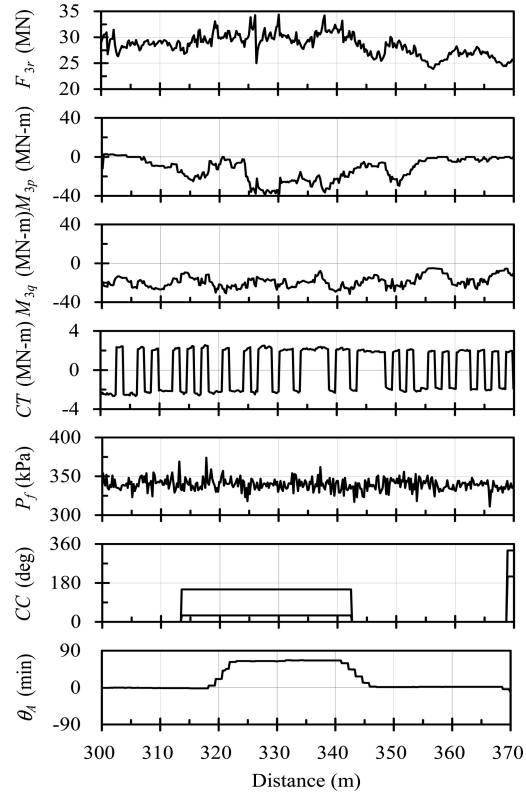

Figure 4. Articulated shield tunnelling operation.

4 SIMULATION OF THE EFFECT OF HARDENED GROUT

The simulation is implemented to predict the articulated shield behaviour based on the in-situ measurement data. The simulations are classified into two main categories, with and without hardened grout between the excavated surface and the extrados of tunnel lining. Four cases of the hardened grout are considered, as shown in Figure 5. The thickness of hardened grout inside the shield tail was assumed to be 30 mm. By applying the articulated shield model, the shield behaviour during excavation can be obtained based on balance of forces acting on the articulated shield.

The dimensions of tunnel and shield, and the shield jack components are shown in Table 1. The tunnel operational control and the tunnel excavation condition shown in Figure 5 are also used in the analysis as input parameters. The effective length of over-excavation, which is the difference between the radius of cutter disc and the radius of shield, and the length of copy cutter used in the simulation are approximately assumed to be 25% and 50% of the actual applications respectively, since the actual applications may not be fully effective during excavation. The selected results of simulations are shown in Figure 6 and can be explained as follows.

The deviations in horizontal directions, Δx (+: downward), the deviations in vertical directions, Δy (+: rightward) and the shield velocity during excavation, v, are plotted for comparison with the observation for all cases. In the first simulation, it is assumed that the hardened grout was not developed in the shield tail (Case 0), of which the results are seemingly correspondent with observations. In the case of the grout intruding into the shield tail, the shield behaviours are gradually changed after the grout hardening up. The shield moved upward for all analysis cases although the hardened grout areas are not the same as shown in Figure 6(a). Case 1 clearly influences the shield deviation in vertical direction, while in Case 2 there is not much effect to the shield deviations. The hardened grout areas affecting the shield deviations in horizontal direction are depicted in Figure 6(b). The shield moved to the right as the hardened grout in the left of the shield tail (Case 3), whereas as the hardened grout in the right of the shield tail, the shield moved to the left (Case 4). In all cases analysed with hardened grout, the changes in the horizontal deviation increase after the shield passes the curved tunnel alignment. This is because the geometric restriction between the shield and the excavated surface is severe at a curved tunnel alignment, whereas the gap between the shield and the

Table 1. Dimension of tunnel, machine used in the analysis.

Item	Component	Value
Tunnel	Horizontal radius	200 m
	Vertical radius	∞ m
	Overburden depth	25.50 m
	Groundwater level	GL-9.00 m
	Outer radius of segment	3.95 m
	Width of segment	1.20 m
Shield	Outer radius	4.04 m
	Total length	8.78 m
	Length of front section	4.45 m
	Length of rear section	4.33 m
	Self-weight	4.73 MN
	Open ratio of cutter face	34.0 %
	Thickness of cutter face	0.55 m
	Radius of chamber	3.51 m
	Length of chamber	1.421 m
	Radius of cutter face	4.055 m
	Cutter disc rotation speed	0.88 rpm
Shield jack	Number of jacks	28
	Cross-sectional area	706.858 cm^2
	Radius of jack	3.66 m
Articulate jack	Number of jacks	20
	Cross-sectional area	865.647 cm^2
	Radius of jack	2.94 m

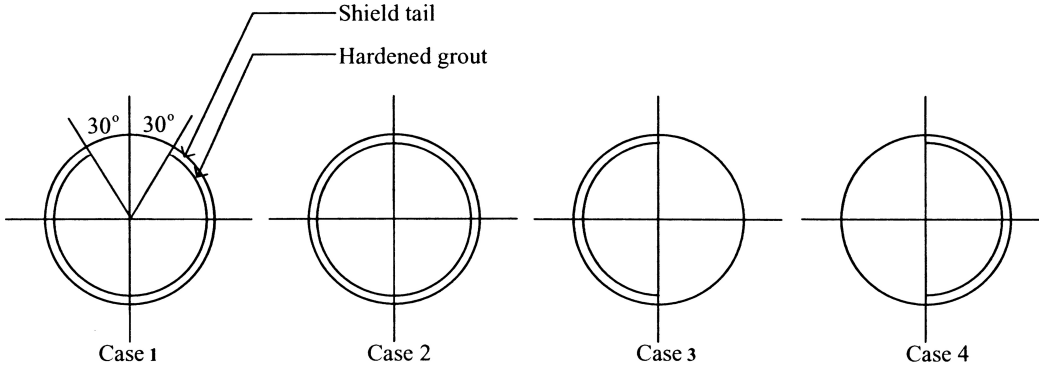

Figure 5. Cases analysed for hardened grout considerations.

excavated surface to rotate the shield easily exists at a straight tunnel alignment. The shield velocities, v, of all analysis cases are very similar in tendency and magnitude as shown in Figure 6(c).

The gaps between the shield and the initial excavated surface, U_n (+: passive state), on both front and rear sections at the curve for Case 0, Case 3 and Case 4 are drawn for comparison as shown in Figure 7. Here, note that the shield periphery is unfolded as a flat plate, i.e., the vertical axis shows the length of the shield and the horizontal axis represents the circumference of the shield. 0° and 180° represent the invert and the crown of the shield respectively, whereas 90° and 270° represent the left and the right spring lines of the shield respectively. As employing the copy cutter between 30° and 150° and the shield rotating to the left, the gap between the shield and the initial excavated surface is largely changed in around spring line. For the front section of Case 0, as shown in Figure 7(a), positive U_n at around the centre of the left spring line is in passive state as the shield skin plate pushes the ground, while in the opposite side (at around the centre of the right spring line), large $|U_n|$ is in active state (negative U_n). Whereas, for the rear section of Case 0, large $|U_n|$ at around the tail of the left spring line is in active state as the ground deforms to the shield skin plate, while in the opposite side (at around the tail of the right spring line), another large U_n is in passive state. U_n in passive and active states for the rear section of Case 3 is at around the left and the right of the spring line respectively as shown in Figure 7(b). This is because when the grout is hardened up in the left of shield tail, the tail clearance in the right side is larger than that in the left side, the shield has to move and rotate to the right to satisfy the equilibrium conditions. On the other hand, U_n of Case 4 is in a similar manner to that of Case 0 as shown in Figure 7(c). This is because the force acting on the shield tail around right spring line changes little, compared with that of Case 0, since the hardened grout at right shield tail does not touch the segment lining during tunnelling at the left curve. But the influence of the hardened grout on the shield tunnelling performance appears after the

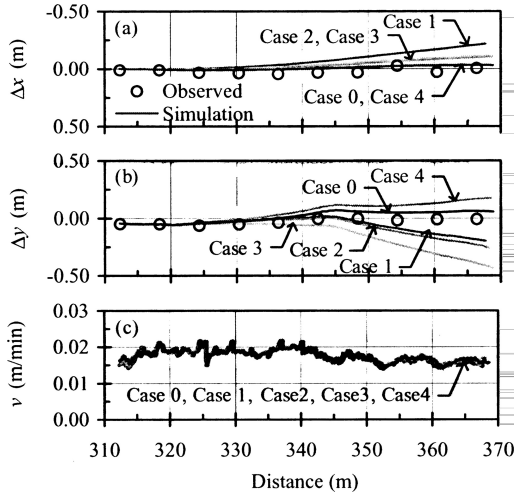

Figure 6. Simulation results.

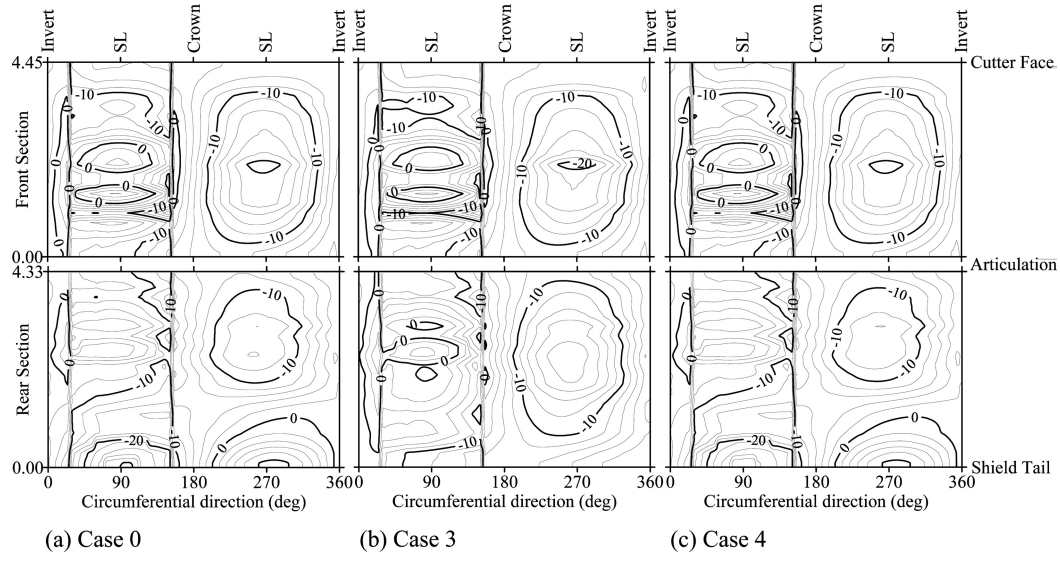

Figure 7. Gap between shield and initial excavated surface.

shield moves to the straight tunnel alignment as shown in Figure 6(b). This means that the influence of the hardened grout on the shield tunnelling performance appears when the tunnel alignment is changed after the grout is intruded and hardened up in the shield tail, since the tail clearance changes less at the same tunnel alignment. U_n shown in Figure 7 are the results of balances of force and moment acting on the shield.

5 CONCLUSIONS

The articulated shield tunnelling at the curved tunnel alignment as well as the influence of grout hardening in the shield tail were simulated. As the result, the conclusions can be made as follows:

1. The articulated shield model can reasonably simulate the articulated shield behaviour during excavation.
2. The articulated angle of the shield is a predominant factor influencing the shield behaviour especially the rotation of shield.
3. The hardening of grout in the shield tail is one of the factors affecting the shield behaviour especially rotation of the shield. Furthermore, the influence of the hardened grout on the shield behaviour appears when the tunnel alignment is changed after the grout is intruded and hardened up in the shield tail.
4. The ground displacement around the shield resulted from the equilibrium condition, which in turn affects the shield behaviour.

REFERENCE

Sugimoto, M. & Sramoon, A. 2002. Theoretical model of shield behavior during excavation I: Theory. *Journal of Geotechnical and Geoenvironmental Engineering* 128(2): 138–155.